

# Two-way conversion of microwave and terahertz radiation into optical fields in Rydberg gases

Martin Kiffner<sup>1,2</sup>, Amir Feizpour<sup>2</sup>, Krzysztof T. Kaczmarek<sup>2</sup>, Dieter Jaksch<sup>2,1</sup>, and Joshua Nunn<sup>2</sup>  
*Centre for Quantum Technologies, National University of Singapore, 3 Science Drive 2, Singapore 117543<sup>1</sup> and  
Clarendon Laboratory, University of Oxford, Parks Road, Oxford OX1 3PU, United Kingdom<sup>2</sup>*

We show that cold Rydberg gases enable an efficient six-wave mixing process where microwave or terahertz fields are coherently converted into optical fields and vice versa. This process is made possible by the long lifetime of Rydberg states, the strong coupling of millimeter waves to Rydberg transitions and a quantum interference effect related to Electromagnetically Induced Transparency. We show that conversion efficiencies within an independent atom approach are of the order of 95% and analyse the impact of dipole-dipole interactions on our scheme. We find that effective conversion efficiencies in the presence of Rydberg-Rydberg interactions can still be as high as 85% based on an implementation with Rubidium atoms. Our frequency conversion scheme does not require cavities and can be implemented for a broad spectrum of terahertz and microwave fields due to the abundance of transitions within the Rydberg manifold.

## I. INTRODUCTION

Two-way conversion of microwave and terahertz radiation into optical fields is a highly desirable capability with numerous applications in classical and quantum technologies. For example, it would enable the metrological transfer of atomic frequency standards [1], novel astronomical surveys [2], long-distance transmission of electronic data via photonic carriers [3], and robust, powerful signal processing for applications in radar and avionics [4]. Efficient conversion of terahertz radiation into visible light would facilitate the detection and imaging of terahertz fields [5, 6]. In the quantum domain, coherent microwave-optical conversion could enable quantum computing via optically-mediated entanglement swapping [7–9] in solid state systems such as spins in silicon [10] or superconducting qubits [11], which lack optical transitions but couple strongly to microwaves. Moreover, Josephson junctions can mediate microwave photonic non-linearities that cannot easily be replicated for optical photons [12] so that coherent microwave-optical conversion also provides a route to freely-scalable all-photonic quantum computing.

Recent proposals for microwave-optical conversion have been based on optomechanical transduction [13–15], or frequency mixing in  $\Lambda$ -type atomic ensembles [16–20]. Both approaches require high quality frequency-selective cavities limiting the conversion bandwidth, as well as aggressive cooling or optical pumping to bring the conversion devices into their quantum ground states.

In this paper, we propose instead to use frequency mixing in Rydberg gases for the conversion of millimeter waves to optical fields (MMOC) (see Fig. 1). In contrast to the conventional definition of millimeter waves, we use this term here for the combined frequency range of terahertz and microwave radiation. Our scheme benefits from the strong coupling between Rydberg atoms and millimeter waves which has previously been used for detection and magnetometry [21–23], storage of microwaves [24] and hybrid atom-photon gates [25]. Here

we show how to achieve efficient and coherent MMOC without the need for cavities, microfabrication or cooling. In contrast to previous frequency mixing schemes in coherent media [26], our system implements a coherent beamsplitter for the two frequency components where an incoming millimeter wave (optical field) is partially or completely converted into an optical field (millimeter wave). This effect is made possible by the long lifetime of the Rydberg states. Our main result is a theoretical model establishing the principle of operation of the proposed device, which it is shown could be implemented in an ensemble of cold trapped Rb atoms.

This paper is organised as follows. We introduce the system and the theoretical model for its description in Sec. II. The results for the conversion of time-independent and pulsed input fields are presented in Sec. III. We discuss the limitations of our scheme due to interactions in Sec. IV, and a brief summary of our work is provided in Sec. V.

## II. MODEL

We consider an ensemble of cold trapped atoms interacting with laser fields and millimeter waves and model these interactions using the standard framework of coupled Maxwell-Bloch equations. A summary of the general approach is presented in Sec. II A, and a detailed derivation can be found in the Supplementary Section ‘Detailed model’. The analytical solution of Maxwell-Bloch equations is outlined in Sec. II B and complemented by the Supplementary Section ‘Methods’.

### A. Maxwell-Bloch equations

In a first step we neglect atom-atom interactions and consider the Bloch equations for a single atom with level scheme as shown in Fig. 1. Imperfections due to interactions are analysed in Sec. IV. The millimeter wave  $\Omega_M$

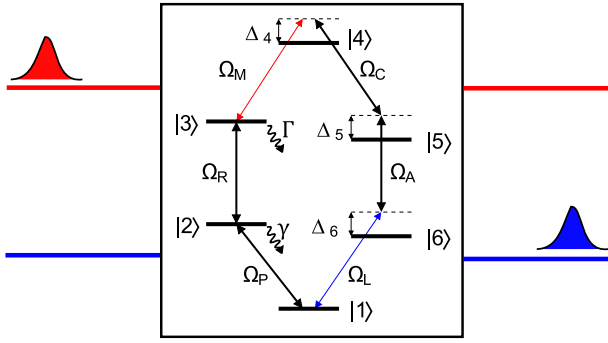


FIG. 1. Schematic drawing of the considered MMOC device. A millimeter wave (red) is coherently converted into an optical field (blue) through the interaction with cold atoms and vice versa. Transition frequencies and detunings shown in the atomic level scheme are not to scale.  $\Omega_M$  and  $\Omega_L$  are the Rabi frequencies associated with the millimeter wave and the laser field, respectively.  $\Omega_P$ ,  $\Omega_R$ ,  $\Omega_C$  and  $\Omega_A$  are Rabi frequencies of the auxiliary fields, and  $\Delta_k$  is the detuning of the fields with state  $|k\rangle$  ( $k \in \{4, 5, 6\}$ ). Levels  $|3\rangle$ ,  $|4\rangle$  and  $|5\rangle$  are Rydberg states with decay rate  $\Gamma \ll \gamma$ , where  $\gamma$  is the decay rate of states  $|2\rangle$  and  $|6\rangle$ .

of interest couples to the transition  $|3\rangle \leftrightarrow |4\rangle$ , where  $|3\rangle$  and  $|4\rangle$  are Rydberg states with principal quantum number  $n \gtrsim 20$ . The optical field  $\Omega_L$  of interest couples to the  $|1\rangle \leftrightarrow |6\rangle$  transition, and the conversion between  $\Omega_M$  and  $\Omega_L$  is facilitated by four auxiliary fields. The resonant fields  $\Omega_P$  and  $\Omega_R$  create a coherence on the  $|1\rangle \leftrightarrow |3\rangle$  transition through coherent population trapping [27]. The two other auxiliary fields  $\Omega_C$  and  $\Omega_A$  are in general off-resonant and establish a coherent connection between the  $|3\rangle \leftrightarrow |4\rangle$  and  $|1\rangle \leftrightarrow |6\rangle$  transitions. We model the time evolution of the atomic density operator by a Markovian master equation

$$\partial_t \rho = -\frac{i}{\hbar} [H, \rho] + \mathcal{L}_\gamma \rho. \quad (1)$$

In electric-dipole and rotating-wave approximation, the Hamiltonian  $H$  in Eq. (1) is given by

$$H = -\hbar \sum_{k=4}^6 \Delta_k A_{kk} - \hbar (\Omega_P A_{21} + \Omega_R A_{32} + \Omega_M A_{43} + \Omega_C A_{45} + \Omega_A A_{56} + \Omega_L A_{61} + \text{H.c.}), \quad (2)$$

and  $A_{ij} = |i\rangle\langle j|$  are atomic transition operators. The detuning  $\Delta_k$  in Eq. (2) is defined as

$$\Delta_4 = \omega_P + \omega_R + \omega_M - \omega_4, \quad (3a)$$

$$\Delta_5 = \omega_P + \omega_R + \omega_M - \omega_C - \omega_5, \quad (3b)$$

$$\Delta_6 = \omega_L - \omega_6, \quad (3c)$$

where  $\hbar\omega_k$  denotes the energy of state  $|k\rangle$  with respect to the energy of level  $|1\rangle$  and  $\omega_X$  is the frequency of field  $X$  with Rabi frequency  $\Omega_X$  ( $X \in \{P, R, C, A, M, L\}$ ). The

term  $\mathcal{L}_\gamma \rho$  in Eq. (1) accounts for spontaneous emission of the excited states. These processes are described by standard Lindblad decay terms. The full decay rate of the states  $|2\rangle$  and  $|6\rangle$  is  $\gamma$ , and the long-lived Rydberg states decay with  $\Gamma \ll \gamma$ . The six fields drive a resonant loop,

$$\omega_P + \omega_R + \omega_M - \omega_C - \omega_A - \omega_L = 0, \quad (4)$$

and we impose the phase matching condition

$$\mathbf{k}_P + \mathbf{k}_R + \mathbf{k}_M - \mathbf{k}_C - \mathbf{k}_A = \mathbf{k}_L. \quad (5)$$

In the following, we assume that  $\Omega_M$  and  $\Omega_L$  are co-propagating, while the directions of the auxiliary fields are chosen such that Eq. (5) holds. Note that this phase matching condition is automatically fulfilled by virtue of Eq. (4) if all fields are co-propagating.

The propagation of the probe and control fields inside the medium is governed by Maxwell's equations. For simplicity we only treat the microwave and laser field in a self-consistent way. The transverse profile of the millimeter wave must not necessarily be confined to the transverse size of the atom cloud, which can be challenging to achieve for millimeter waves. If the transverse waist of the millimeter wave exceeds the atomic cloud dimensions, the effective one-dimensional situation considered here can be realised by confining the millimeter wave to a waveguide such that its principal transverse electric mode significantly overlaps with the atomic cloud. In the slowly varying envelope approximation we find

$$\left(\frac{1}{c}\partial_t + \partial_z\right)\Omega_M = i\eta_M \rho_{43}, \quad (6a)$$

$$\left(\frac{1}{c}\partial_t + \partial_z\right)\Omega_L = i\eta_L \rho_{61}. \quad (6b)$$

The coupling constants  $\eta_M$  and  $\eta_L$  are given by

$$\eta_M = \frac{\mathcal{N}|\mathbf{d}_{43}|^2}{2\hbar\epsilon_0 c}\omega_M, \quad (7a)$$

$$\eta_L = \frac{\mathcal{N}|\mathbf{d}_{61}|^2}{2\hbar\epsilon_0 c}\omega_L, \quad (7b)$$

where

$$\mathbf{d}_{kl} = \langle k|\hat{\mathbf{d}}|l\rangle \quad (8)$$

is the matrix element of the electric dipole moment operator  $\hat{\mathbf{d}}$  on the transition transition  $|k\rangle \leftrightarrow |l\rangle$ ,  $c$  is the speed of light and  $\mathcal{N}$  is the atomic density of the medium. The ratio of the coupling constants can be expressed in terms of the ratio  $b = g_M/g_L$  of the single photon Rabi frequencies  $g_M$  and  $g_L$ ,

$$b^2 = (g_M/g_L)^2 = \eta_M/\eta_L, \quad (9)$$

where  $g_M$  ( $g_L$ ) corresponds to the  $|3\rangle \leftrightarrow |4\rangle$  ( $|1\rangle \leftrightarrow |6\rangle$ ) transition. The set of equations (1) and (6) represent a system of coupled, partial differential equations and have

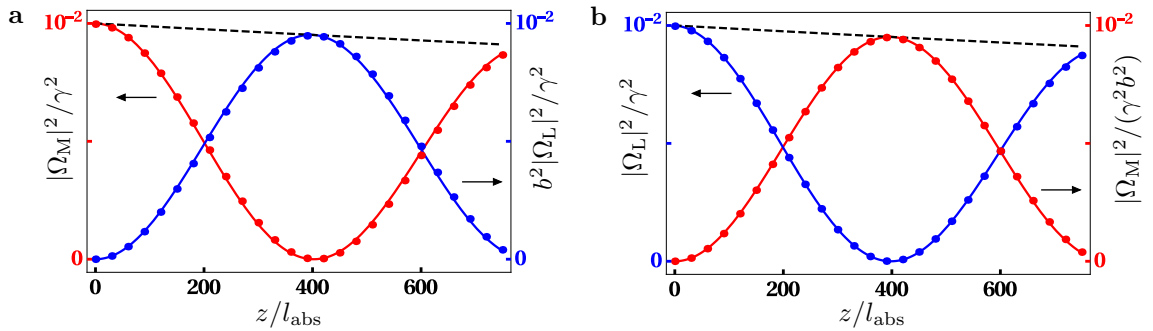


FIG. 2. Frequency conversion of stationary fields. Intensities of the millimeter wave (red) and optical field (blue) inside the medium. Dots indicate the results from a numerical integration of Maxwell-Bloch equations (see Methods). **a** A CW millimeter wave enters the medium at  $z = 0$ . **b** A CW optical field enters the medium at  $z = 0$ . In **a** and **b**, the dashed line is proportional to the envelope  $e^{-2\kappa z}$  and we set  $\Gamma/\gamma = 10^{-3}$ ,  $\Omega_A = 2\gamma$ ,  $\Omega_C = 2\gamma$ ,  $\Omega_R = 2\gamma$ ,  $\Omega_P = 0.063\gamma$ ,  $\Delta_4 = 2\gamma$ ,  $\Delta_5 = 2\gamma$ ,  $\Delta_6 = 2\gamma$  and  $b = 1$ .

to be solved consistently for given initial and boundary conditions. We numerically solve the semi-classical system in Eqs. (1) and (6) using MATHEMATICA [28] and the implicit differential-algebraic solver (IDA) method option for NDSolve.

### B. Analytical solution

Here we outline the derivation of an analytical solution to the coupled Maxwell-Bloch equations (1) and (6). To this end, we follow the approach in [29, 30] and find the first order solution of Eq. (1) with respect to the Rabi frequencies  $\Omega_M$  and  $\Omega_L$ . The resulting density matrix is too complicated to give here, but the matrix elements  $\varrho_{43}$  and  $\varrho_{61}$  entering Eq. (6) have the general form

$$\varrho_{43} \approx \chi_{43}^{(M)} \Omega_M + \chi_{43}^{(L)} \Omega_L, \quad (10a)$$

$$\varrho_{61} \approx \chi_{61}^{(M)} \Omega_M + \chi_{61}^{(L)} \Omega_L. \quad (10b)$$

The response of the atomic system on the  $|3\rangle \leftrightarrow |4\rangle$  transition induced by the millimeter wave is described by  $\chi_{43}^{(M)}$ , and  $\chi_{61}^{(L)}$  accounts for the atomic response on the transition  $|1\rangle \leftrightarrow |6\rangle$  due to the optical field. In addition, the millimeter wave can induce a coherence proportional to  $\chi_{61}^{(M)}$  on the optical transition  $|1\rangle \leftrightarrow |6\rangle$ , and the optical field can create a coherence proportional to  $\chi_{43}^{(L)}$  on the transition  $|3\rangle \leftrightarrow |4\rangle$ . The cross-terms proportional to  $\chi_{43}^{(L)}$  and  $\chi_{61}^{(M)}$  in Eq. (10) originate from the closed-loop character of the atomic level scheme and are responsible for the interconversion of the millimeter and optical waves as discussed in Sec. III.

Next we combine Eq. (10) with Eq. (6) and assume that the millimeter and optical waves are time independent. We thus obtain the following ordinary differential equation,

$$\partial_z \Omega = i\mathcal{M}\Omega, \quad (11)$$

where

$$\mathcal{M} = \eta_L \begin{pmatrix} b^2 \chi_{43}^{(M)} & b^2 \chi_{43}^{(L)} \\ \chi_{61}^{(M)} & \chi_{61}^{(L)} \end{pmatrix}, \quad \Omega = \begin{pmatrix} \Omega_M \\ \Omega_L \end{pmatrix}. \quad (12)$$

The general solution to Eq. (11) is

$$\Omega = \exp(i\mathcal{M}z)\Omega_0, \quad (13)$$

and  $\Omega_0$  is  $\Omega$  evaluated at  $z = 0$ . An analytical expression for the matrix exponential in Eq. (13) can be obtained, e.g., by expanding  $\mathcal{M}$  in terms of the  $2 \times 2$  identity matrix and the Pauli matrices as shown in the Supplementary Section 'Methods'.

The analytical solution presented here treats the fields  $\Omega_M$  and  $\Omega_L$  as  $c$ -numbers. However, the generalisation to quantum fields is straightforward since the coherences in Eq. (10) are linear in the Rabi frequencies  $\Omega_M$  and  $\Omega_L$ . Apart from quantum noise operators, our calculations are thus equivalent to a Heisenberg-Langevin approach where the Rabi frequencies  $\Omega_M$  and  $\Omega_L$  are replaced by quantum fields [31–33]. Since the Langevin noise operators represent only vacuum noise, they do not contribute to normally ordered expectation values like the intensity.

### III. RESULTS

In a first step we consider the interconversion of time-independent fields investigated in Sec. II B. In general, the conversion between millimeter waves and optical fields according to Eq. (13) will be small for a generic matrix  $\mathcal{M}$ . However, investigating the general solution in Eq. (13) shows that efficient and coherent conversion can be achieved if the diagonal elements of  $\mathcal{M}$  vanish, i.e.,  $\chi_{43}^{(M)} \approx \chi_{61}^{(L)} \approx 0$ . In this case, a weak millimeter wave  $\Omega_M$  creates a coherence on the optical transition  $|6\rangle \leftrightarrow |1\rangle$ , but not on the  $|4\rangle \leftrightarrow |3\rangle$  transition. Similarly, a weak laser field  $\Omega_L$  creates a coherence on the

$|4\rangle \leftrightarrow |3\rangle$  transition without generating a coherence on the  $|6\rangle \leftrightarrow |1\rangle$  transition. We find that the conditions  $\chi_{43}^{(M)} \approx \chi_{61}^{(L)} \approx 0$  can indeed be met in our system if the intensities and detunings of the auxiliary fields obey the following conditions,

$$|\Omega_R| \gg |\Omega_P|, \quad \Delta_5 = \frac{|\Omega_C|^2}{\Delta_4}, \quad \Delta_6 = \frac{|\Omega_A|^2}{\Delta_5}. \quad (14)$$

This result can be understood as follows. The level scheme in Fig. 1 can be regarded as three consecutive EIT systems where the weak probe fields are represented by  $\Omega_P$ ,  $\Omega_M$  and  $\Omega_L$ , respectively. However, these three systems are coupled and hence the normal two-photon resonance condition for transparency of the  $\Omega_M$  and  $\Omega_L$  fields is changed. The conditions in Eq. (14) approximately restore transparency for the field  $\Omega_M$  ( $\Omega_L$ ) on the transition  $|3\rangle \leftrightarrow |4\rangle$  ( $|1\rangle \leftrightarrow |6\rangle$ ) and in the presence of the other levels and fields. However,  $\Omega_M$  still creates a coherence on the optical transition and  $\Omega_L$  induces a coherence on the Rydberg transition such that the fields are inter-converted as they propagate along the medium. With Eq. (14) the general solution for the spatial distribution of the fields in Eq. (13) is given by (see Supplementary Section ‘Methods’)

$$\mathbf{\Omega}(z) \approx e^{-\kappa z} \begin{pmatrix} \cos(kz) & ib \sin(kz) \\ \frac{i}{b} \sin(kz) & \cos(kz) \end{pmatrix} \mathbf{\Omega}(0), \quad (15)$$

where  $\kappa = (\varepsilon^2 + \varepsilon_\Gamma)/l_{\text{abs}}$  and  $k = \varepsilon/l_{\text{abs}}$  determine the loss and the spatial oscillation period of the interconversion, respectively, and  $l_{\text{abs}} = \gamma/(4\eta_L)$  is the resonant absorption length on the  $|6\rangle \leftrightarrow |1\rangle$  transition. The dimensionless parameters  $\varepsilon$  and  $\varepsilon_\Gamma$  are defined as

$$\varepsilon = \frac{b}{4} \frac{\gamma}{|\Delta_4|} \frac{|\Omega_C| |\Omega_P|}{|\Omega_A| |\Omega_R|}, \quad \varepsilon_\Gamma = \frac{\Gamma\gamma}{16|\Omega_A|^2} \left( 1 + 2 \frac{|\Omega_C|^2}{\Delta_4^2} \right), \quad (16)$$

and we assumed  $\varepsilon \ll 1$  and  $\varepsilon_\Gamma/\varepsilon \ll 1$ . In Eq. (15), the off-diagonal matrix element (1, 2) [ $(2, 1)$ ] is proportional to  $b$  ( $1/b$ ) since a single optical (microwave/terahertz) photon with Rabi frequency  $g_L$  ( $g_M$ ) gives rise to a Rabi frequency  $bg_L$  ( $g_M/b$ ) on the microwave/terahertz (optical) transition.

The spatial oscillations of optical and millimeter wave intensities according to Eq. (15) are shown in Fig. 2. Our simple model is in excellent agreement with a full numerical solution of Maxwell-Bloch equations. Complete MMOC occurs after a length  $L_c = \pi/(2k)$ , and thus requires an optical depth  $D_c = L_c/l_{\text{abs}}$  that is inversely proportional to  $\varepsilon$  in Eq. (16),  $D_c = \pi/(2\varepsilon)$ . Since the value of  $\varepsilon$  can be adjusted through the intensities and frequencies of the auxiliary fields, the condition for complete MMOC can be met for various densities and sizes of atomic gases. In the example in Fig. 2, we find  $L_c \approx 400l_{\text{abs}}$ . The fidelity  $F = e^{-2\kappa L_c}$  for complete conversion can be expressed in terms of the optical depth

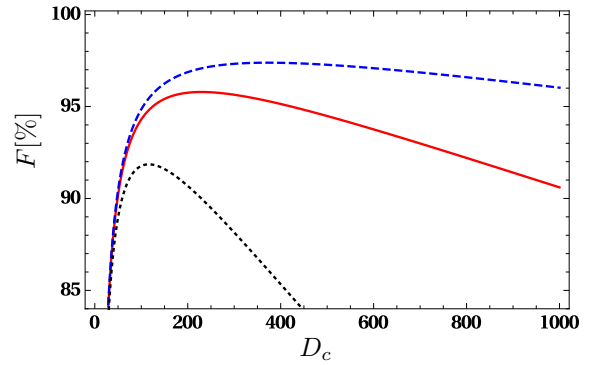


FIG. 3. Conversion fidelity as a function of optical depth  $D_c$ . We set  $\Gamma/\gamma = 3.9 \times 10^{-3}$  (black dotted line),  $\Gamma/\gamma = 10^{-3}$  (red solid line) and  $\Gamma/\gamma = 3.8 \times 10^{-4}$  (blue dashed line). These parameters correspond to Rubidium Rydberg states at zero temperature with  $n \approx 20$ ,  $n \approx 30$  and  $n \approx 40$ , respectively. Common parameters in all three curves are  $\Omega_A = 2\gamma$ ,  $\Omega_C = 2\gamma$  and  $\Delta_4 = 2\gamma$ .

$D_c$ ,

$$F(D_c) = \exp \left[ -\frac{\pi^2}{2D_c} \right] \exp [-2\varepsilon_\Gamma D_c], \quad (17)$$

and  $F(D_c)$  is shown in Fig. 3 for three different values of  $\varepsilon_\Gamma$ . The maximum fidelity  $F_{\text{max}} = \exp(-2\pi\sqrt{\varepsilon_\Gamma})$  is attained at an optical depth  $D_c^{\text{max}} = \pi/(2\sqrt{\varepsilon_\Gamma})$  and tends to unity for  $\varepsilon_\Gamma \rightarrow 0$ . Since  $\varepsilon_\Gamma \propto \Gamma$ , fidelities close to unity are only possible because of the slow radiative decay rate  $\Gamma$  of the Rydberg levels  $|3\rangle$ ,  $|4\rangle$  and  $|5\rangle$ .  $\Gamma$  decreases with increasing  $n$  as  $\Gamma \propto n^{-3}$  [34] and is thus typically several orders of magnitude smaller than the decay rate  $\gamma$  of the low-lying states  $|2\rangle$  and  $|6\rangle$ . The fidelity for complete MMOC for the parameters in Fig. 2 is  $F \approx 95.1\%$ . In the Supplementary Section ‘Example system’ we discuss a possible realisation of our level scheme in  $^{87}\text{Rb}$ . We find that the fidelity for MMOC and the required optical depth  $D_c$  for complete conversion are very similar to the results presented in Fig. 2.

Next we consider the conversion of pulsed fields. The derivation of Eq. (15) shows that our scheme is not mode-selective and works for broadband pulses. The only requirement is that the atomic dynamics remains in the adiabatic regime, which holds if the bandwidth  $\delta\nu$  of the input pulse is smaller than all detunings  $\Delta_k$  and the Rabi frequencies  $\Omega_R$ ,  $\Omega_C$  and  $\Omega_A$  (see Supplementary Section ‘Methods’). In order to demonstrate this, we present numerical solutions of Maxwell-Bloch equations for a millimeter wave input pulse as shown in Fig. 4. The intensity of a millimeter wave input pulse with Gaussian envelope is shown in Fig. 4a, and the corresponding optical output field is shown in Fig. 4b. The input pulse has a bandwidth of the order of  $\Delta\nu \approx 2\pi \times 80\text{kHz}$  and is converted without distortion of its shape. We thus find that the bandwidth of our conversion scheme is at least of the order of 80kHz for the chosen parameters. This bandwidth

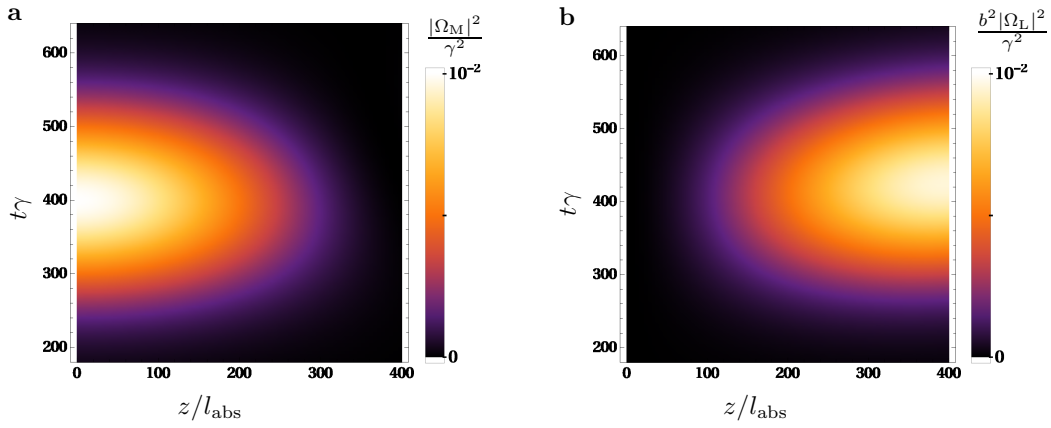


FIG. 4. Frequency conversion of pulsed fields. **a** Density plot of the incoming millimeter wave pulse with a Gaussian envelope. **b** Density plot of the outgoing optical pulse. The parameters in **a** and **b** are the same as in Fig. 2.

can be significantly increased by increasing the detunings and Rabi frequencies of the auxiliary fields. Finally, we note that the conversion of optical pulses to millimeter waves works equally well.

#### IV. INTERACTION-INDUCED IMPERFECTIONS

The results in the previous Section III show that coherent MMOC with very high conversion efficiencies is possible in cold atomic ensembles with large optical depth. However, our model is based on non-interacting atoms, but Rydberg atoms interact strongly via dipole-dipole interactions. It is thus crucial to analyse the impact of Rydberg-Rydberg interaction on MMOC and to identify parameter regimes where the independent atom approximation holds.

A key part of our scheme is the phenomenon of coherent population trapping in state  $|3\rangle$  via the ladder system  $|1\rangle \leftrightarrow |2\rangle \leftrightarrow |3\rangle$ . Several interaction effects can disturb or even destroy this effect. First, van der Waals interactions between pairs of Rydberg atoms lead to energy shifts  $\Delta_{\text{vdW}}$  of state  $|3\rangle$ . If this shift is large or comparable to the EIT linewidth, the P field will be absorbed by atoms within the blockade radius of the Rydberg excitation [35]. Second, cooperative effects like superradiance [36] can transfer population from  $|3\rangle$  to unwanted states thus destroying the coherent population trapping effect. Third, a ground state atom within the electron orbit of a Rydberg state can shift the energy of the Rydberg level [37] such that EIT is destroyed and the P field is absorbed. However, experimental results [35, 38, 39] show that near-perfect EIT based on single-atom physics can be observed in Rydberg systems with principal quantum numbers  $n \lesssim 40$  and for weak probe fields such that the population of the Rydberg state is small.

An additional requirement for the validity of our independent atom model is that all interaction-induced frequency

shifts of the atomic levels are small as compared to the bandwidth of the conversion mechanism. The Rydberg states of our level scheme experience van der Waals shifts  $\Delta_{\text{vdW}}$  as well as frequency shifts induced by the resonant dipole-dipole interaction  $\Delta_{\text{DD}}$  [40]. For example, if states  $|3\rangle$  and  $|4\rangle$  correspond to  $ns$  and  $np$  states, respectively, the dipole-dipole interaction couples the two-atom states  $|3, 4\rangle$  and  $|4, 3\rangle$  thus leading to energy shifts of the resulting dressed states. Note that the magnitude of  $\Delta_{\text{DD}}$  depends crucially on the quantum numbers of the involved states.

In the Supplementary Section 'Level shifts' we estimate the magnitude of  $\Delta_{\text{vdW}}$  and  $\Delta_{\text{DD}}$  for different principal quantum numbers  $n$ . To this end, we evaluate  $\Delta_{\text{vdW}}$  and  $\Delta_{\text{DD}}$  for two Rb atoms separated by  $R_{90}$ , where  $R_{90}$  is the distance such that 90% of all Rydberg excitations in the ensemble have a distance  $r > R_{90}$ . If  $\Delta_{\text{vdW}}$  and  $\Delta_{\text{DD}}$  are smaller than the conversion bandwidth, at least 90% of all atoms contribute to the conversion mechanism and hence we expect that the effective efficiency is  $0.9 \times F$ , where  $F$  is the fidelity based on the single-atom analysis. For an atomic density of  $\mathcal{N} = 3 \times 10^{17} \text{m}^{-3}$  and a Rydberg excitation probability of  $10^{-3}$ , we find that  $\Delta_{\text{vdW}}$  and  $\Delta_{\text{DD}}$  are at most of the order of 100kHz for  $n \leq 40$  and if the Rydberg states  $|3\rangle$  and  $|4\rangle$  correspond to  $(n-1)s$  and  $np$  states, respectively. If  $|3\rangle \leftrightarrow |4\rangle$  is a transition between  $ns$  and  $np$  states with the same principal quantum number,  $\Delta_{\text{DD}}$  is of the order of 150kHz for  $n = 20$  and 3MHz for  $n = 40$ . While conversion bandwidths of several MHz may require very large optical depths and high laser intensities, conversion bandwidths of the order of several 100kHz should be feasible. In particular, we show in the Supplementary Section 'Example system' that the parameters in Sec. III can be realised with Rb atoms where the Rydberg states  $|3\rangle$  and  $|4\rangle$  are  $29S$  and  $30P$  states, respectively. In this case,  $\Delta_{\text{vdW}}$  and  $\Delta_{\text{DD}}$  are smaller than the bandwidth of the conversion mechanism and hence conversion with effective fidelities exceeding 85% can be realised.

## V. SUMMARY

We have shown that frequency mixing in Rydberg gases enables the coherent conversion between millimeter waves and optical fields. The degree of conversion can be adjusted through the atomic density and the ancillary drive field intensities and frequencies. Complete conversion for travelling waves is achieved within a few hundred absorption lengths, and conversion fidelities of our scheme can exceed 95%. Imperfections of our scheme due to atom-atom interactions can be minimised in ensembles with low atomic densities and by the choice of the atomic states and parameters of the auxiliary fields. Even if losses due to interactions are taken into account, we estimate that conversion efficiencies can still be as high as 85% or more. Due to the abundant possibilities

for choosing the  $|3\rangle \leftrightarrow |4\rangle$  transition within the Rydberg manifold, our proposed MMOC scheme enables the conversion of various frequencies ranging from terahertz radiation to the high-frequency part of the microwave spectrum. We have shown that our scheme can be implemented in an ensemble of Rb atoms and hence we are confident that it can be realised with existing technology and in the near future.

## ACKNOWLEDGMENTS

We thank the National Research Foundation and the Ministry of Education of Singapore for support. The research leading to these results has received funding from the European Research Council under the European Unions Seventh Framework Programme (FP7/2007-2013)/ERC Grant Agreement no. 319286 Q-MAC.

- 
- [1] T. Fortier, M. Kirchner, F. Quinlan, J. Taylor, J. Bergquist, T. Rosenband, N. Lemke, A. Ludlow, Y. Jiang, C. Oates, *et al.*, *Nat. Photon.* **5**, 425 (2011)
  - [2] R. Martin, C. Schuetz, T. Dillon, D. Mackrides, P. Yao, K. Shreve, C. Harrity, A. Zablocki, B. Overmiller, P. Curt, *et al.*, *SPIE Newsroom*, Aug(2012)
  - [3] X. Yang, K. Xu, J. Yin, Y. Dai, F. Yin, J. Li, H. Lu, T. Liu, and Y. Ji, *OPTEXP* **22**, 869 (2014)
  - [4] M. Loïc, C. Stéphanie, F. Christian, C. Jean, M. Thomas, P. Gregoire, B. Ghaya, A. Mehdi, D. Daniel, B. Fabien, *et al.*, in *Radar Conference-Surveillance for a Safer World, 2009. RADAR. International* (IEEE, 2009) pp. 1–5
  - [5] A. J. L. Adam, *J. Infrared Milli. Terahz. Waves* **32**, 976 (2011)
  - [6] W. L. Chan, J. Deibel, and D. M. Mittleman, *Rep. Prog. in Phys.* **70**, 1325 (2007)
  - [7] S. D. Barrett and P. Kok, *Phys. Rev. A* **71**, 060310 (2005)
  - [8] C. Monroe, R. Raussendorf, A. Ruthven, K. Brown, P. Maunz, L.-M. Duan, and J. Kim, *Phys. Rev. A* **89**, 022317 (2014)
  - [9] K. Nemoto, M. Trupke, S. J. Devitt, A. M. Stephens, B. Scharfenberger, K. Buczak, T. Nöbauer, M. S. Everitt, J. Schmiedmayer, and W. J. Munro, *Phys. Rev. X* **4**, 031022 (2014)
  - [10] J. J. Morton and K. Mølmer, *Nature* **517**, 153 (2015)
  - [11] R. Barendst, J. Kelly, A. Megrant, A. Veitia, D. Sank, E. Jeffrey, T. White, J. Mutus, A. Fowler, B. Campbell, Y. Chen, Z. Chen, B. Chiaro, A. Dunsworth, C. Neill, P. O'Malley, P. Roushan, A. Vainsencher, J. Wenner, A. N. Korotkov, A. N. Cleland, and J. M. Martinis, *Nature* **508**, 500 (2014)
  - [12] A. Wallraff, D. I. Schuster, A. Blais, L. Frunzio, R.-S. Huang, J. Majer, S. Kumar, S. M. Girvin, and R. J. Schoelkopf, *Nature* **431**, 162 (2004)
  - [13] R. Andrews, R. Peterson, T. Purdy, K. Cicak, R. Simmonds, C. Regal, and K. Lehnert, *Nat. Phys.* **10**, 321 (2014)
  - [14] T. Bagci, A. Simonsen, S. Schmid, L. G. Villanueva, E. Zeuthen, J. Appel, J. M. Taylor, A. Sørensen, K. Usami, A. Schliesser, *et al.*, *Nature* **507**, 81 (2014)
  - [15] K. Xia, M. R. Vanner, and J. Twamley, *Sci. Rep.* **4**, 5571 (2014)
  - [16] L. A. Williamson, Y.-H. Chen, and J. J. Longdell, *Phys. Rev. Lett.* **113**, 203601 (2014)
  - [17] C. O'Brien, N. Lauk, S. Blum, G. Morigi, and M. Fleischhauer, *Phys. Rev. Lett.* **113**, 063603 (2014)
  - [18] S. Blum, C. O'Brien, N. Lauk, P. Bushev, M. Fleischhauer, and G. Morigi, *Phys. Rev. A* **91**, 033834 (2015)
  - [19] M. Hafezi, Z. Kim, S. Rolston, L. Orozco, B. Lev, and J. Taylor, *Phys. Rev. A* **85**, 020302 (2012)
  - [20] D. Marcos, M. Wubs, J. Taylor, R. Aguado, M. Lukin, and A. S. Sørensen, *Phys. Rev. Lett.* **105**, 210501 (2010)
  - [21] J. A. Sedlacek, A. Schwettmann, H. Kübler, R. Löw, T. Pfau, and J. P. Shaffer, *Nat. Phys.* **8**, 819 (2012)
  - [22] J. A. Gordon, C. L. Holloway, A. Schwarzkopf, D. A. Anderson, S. Miller, N. Thaicharoen, and G. Raithel, *Appl. Phys. Lett.* **105**, 024104 (2014)
  - [23] H. Fan, S. Kumar, J. Sedlacek, H. Kübler, S. Karimkashi, and J. P. Shaffer, *J. Phys. B* **48**, 202001 (2015)
  - [24] D. Petrosyan, G. Bentsky, G. Kurizki, I. Mazets, J. Majer, and J. Schmiedmayer, *Phys. Rev. A* **79**, 040304(R) (2009)
  - [25] J. D. Pritchard, J. A. Isaacs, M. A. Beck, R. McDermott, and M. Saffman, *Phys. Rev. A* **89**, 010301(R) (2014)
  - [26] M. Fleischhauer, A. Imamoglu, and J. P. Marangos, *Rev. Mod. Phys.* **77**, 633 (2005)
  - [27] E. Arimondo, in E. Wolf (Ed.), *Progress in Optics*, Vol. **35**, pp. 258, Elsevier, Amsterdam (1996).
  - [28] Wolfram Research, Inc., *Mathematica Version 10.1* (Wolfram Research, Inc., Irvine, Champaign, Illinois)
  - [29] M. Kiffner and K.-P. Marzlin, *Phys. Rev. A* **71**, 033811 (2005)
  - [30] M. Kiffner, U. Dorner, and D. Jaksch, *Phys. Rev. A* **85**, 023812 (2012)
  - [31] M. Fleischhauer and M. D. Lukin, *Phys. Rev. A* **65**, 022314 (2002)
  - [32] M. Hafezi, D. E. Chang, V. Gritsev, E. Demler, and M. Lukin, *Phys. Rev. B* **85**, 013822 (2012)
  - [33] F. E. Zimmer, J. Otterbach, R. G. Unanyan, B. W. Shore, and M. Fleischhauer, *Phys. Rev. A* **77**, 063823 (2008)

- [34] I. I. Beterov, I. I. Ryabtsev, D. B. Tretyakov, and V. M. Entin, *Phys. Rev. A* **79**, 052504 (2009)
- [35] J. D. Pritchard and K. J. Weatherill and C. S. Adams, in *Annual Review of Cold Atoms and Molecules*, edited by K. Madison, Y. Wang, A. M. Rey, and K. Bongs, (World Scientific, Singapore, 2013), Vol. **1**, pp. 301.
- [36] T. Wang, S. F. Yelin, R. Cote, E. E. Eyler, S. M. Farooqi, P. L. Gould, M. Kostrun, D. Tong, and D. Vrinceanu, *Phys. Rev. A* **75**, 033802 (2007)
- [37] V. Bendkowsky, B. Butscher, J. N. J. P. Shaffer, R. Löw, and T. Pfau, *Nature* **458**, 1005 (2009)
- [38] K. J. Weatherill, J. D. Pritchard, R. P. Abel, M. G. Bason, A. K. Mohapatra, and C. S. Adams, *J. Phys. B* **41**, 201002 (2008)
- [39] J. Han, T. Vogt, M. Manjappa, R. Guo, M. Kiffner, and W. Li, *Phys. Rev. A* **92**, 063824 (2015)
- [40] T. F. Gallagher, *Rydberg Atoms* (Cambridge University Press, Cambridge, 1994)

## Supplemental Material for:

# Two-way conversion of microwave and terahertz radiation into optical fields in Rydberg gases

## VI. DETAILED MODEL

Here we derive the Maxwell-Bloch equations for our system from first principles. The electric field amplitude of the millimeter wave is  $\mathbf{E}_M$ , and the optical field is denoted by  $\mathbf{E}_L$ . The other fields  $\mathbf{E}_P$ ,  $\mathbf{E}_R$  and  $\mathbf{E}_C$  are auxiliary fields facilitating the frequency conversion. We decompose all electric fields as ( $X \in \{P, R, M, C, L\}$ )

$$\mathbf{E}_X = \mathbf{E}_X^{(+)}(\mathbf{r}, t) + \text{c.c.}, \quad (18)$$

where  $\mathbf{E}_X^{(+)}$  is the positive frequency part of field X. The positive frequency parts of  $\mathbf{E}_M$  and  $\mathbf{E}_L$  are defined as

$$\mathbf{E}_M^{(+)}(\mathbf{r}, t) = \mathbf{e}_M \mathcal{E}_M(\mathbf{r}, t) e^{i(\mathbf{k}_M \cdot \mathbf{r} - \omega_M t)}, \quad (19a)$$

$$\mathbf{E}_L^{(+)}(\mathbf{r}, t) = \mathbf{e}_L \mathcal{E}_L(\mathbf{r}, t) e^{i(\mathbf{k}_L \cdot \mathbf{r} - \omega_L t)}, \quad (19b)$$

where  $\mathbf{e}_M$  ( $\mathbf{e}_L$ ) is the unit polarisation vector,  $\omega_M$  ( $\omega_L$ ) is the central frequency,  $\mathbf{k}_M$  ( $\mathbf{k}_L$ ) is the wave vector and  $\mathcal{E}_M$  ( $\mathcal{E}_L$ ) is the envelope function of  $\mathbf{E}_M$  ( $\mathbf{E}_L$ ). The positive frequency parts of the auxiliary fields are given by

$$\mathbf{E}_P^{(+)}(\mathbf{r}, t) = \mathbf{e}_P \mathcal{E}_P e^{i(\mathbf{k}_P \cdot \mathbf{r} - \omega_P t)}, \quad (20a)$$

$$\mathbf{E}_R^{(+)}(\mathbf{r}, t) = \mathbf{e}_R \mathcal{E}_R e^{i(\mathbf{k}_R \cdot \mathbf{r} - \omega_R t)}, \quad (20b)$$

$$\mathbf{E}_C^{(+)}(\mathbf{r}, t) = \mathbf{e}_C \mathcal{E}_C e^{i(\mathbf{k}_C \cdot \mathbf{r} - \omega_C t)}, \quad (20c)$$

$$\mathbf{E}_A^{(+)}(\mathbf{r}, t) = \mathbf{e}_A \mathcal{E}_A e^{i(\mathbf{k}_A \cdot \mathbf{r} - \omega_A t)}, \quad (20d)$$

where  $\mathbf{e}_X$ ,  $\mathcal{E}_X$  and  $\omega_X$  is the unit polarisation vector, envelope function and central frequency of field  $\mathbf{E}_X$ , respectively ( $X \in \{P, R, C, A\}$ ). In order to simplify the notation, we introduce atomic transition operators

$$A_{kl} = |k\rangle\langle l|, \quad A_{kl}^\dagger = A_{lk}. \quad (21)$$

In electric-dipole and rotating-wave approximation, the Hamiltonian of each atom interacting with the six laser fields is

$$\begin{aligned} \tilde{H} = & \hbar \sum_{k=2}^5 \omega_k A_{kk} - \left( A_{21} \mathbf{d}_{21} \cdot \mathbf{E}_P^{(+)} + A_{32} \mathbf{d}_{32} \cdot \mathbf{E}_R^{(+)} \right. \\ & + A_{43} \mathbf{d}_{43} \cdot \mathbf{E}_M^{(+)} + A_{45} \mathbf{d}_{45} \cdot \mathbf{E}_C^{(+)} \\ & \left. + A_{56} \mathbf{d}_{56} \cdot \mathbf{E}_A^{(+)} + A_{61} \mathbf{d}_{61} \cdot \mathbf{E}_L^{(+)} + \text{H.c.} \right), \quad (22) \end{aligned}$$

where  $\hbar\omega_k$  denotes the energy of state  $|k\rangle$  with respect to the energy of level  $|1\rangle$ . The matrix element of the electric

dipole moment operator  $\hat{\mathbf{d}}$  on the transition transition  $|k\rangle \leftrightarrow |l\rangle$  is defined as

$$\mathbf{d}_{kl} = \langle k | \hat{\mathbf{d}} | l \rangle. \quad (23)$$

We model the time evolution of the atomic system by a master equation for the reduced density operator  $R$ ,

$$\partial_t R = -\frac{i}{\hbar} [\tilde{H}, R] + \mathcal{L}_\gamma R. \quad (24)$$

The last term in Eq. (24) describes spontaneous emission and is given by

$$\begin{aligned} \mathcal{L}_\gamma R = & -\frac{\gamma}{2} \left( A_{12}^\dagger A_{12} R + R A_{12}^\dagger A_{12} - 2A_{12} R A_{12}^\dagger \right) \\ & -\frac{\Gamma}{2} \left( A_{23}^\dagger A_{23} R + R A_{23}^\dagger A_{23} - 2A_{23} R A_{23}^\dagger \right), \\ & -\frac{\Gamma}{2} \left( A_{34}^\dagger A_{34} R + R A_{34}^\dagger A_{34} - 2A_{34} R A_{34}^\dagger \right), \\ & -\frac{\Gamma}{2} \left( A_{54}^\dagger A_{54} R + R A_{54}^\dagger A_{54} - 2A_{54} R A_{54}^\dagger \right), \\ & -\frac{\Gamma}{2} \left( A_{65}^\dagger A_{65} R + R A_{65}^\dagger A_{65} - 2A_{65} R A_{65}^\dagger \right). \\ & -\frac{\gamma}{2} \left( A_{16}^\dagger A_{16} R + R A_{16}^\dagger A_{16} - 2A_{16} R A_{16}^\dagger \right). \end{aligned}$$

While the ground states  $|1\rangle$  is assumed to be (meta-) stable, the states  $|2\rangle$ ,  $|3\rangle$ ,  $|4\rangle$  and  $|5\rangle$  decay through spontaneous emission. The decay rate  $\gamma$  is the full decay rate of states  $|2\rangle$  and  $|5\rangle$ , and  $\Gamma$  is the decay rate on the Rydberg transitions. In our scheme,  $\Gamma$  is much smaller than the decay rate  $\gamma$  of the low-lying electronic states. In order to remove the fast oscillating terms in Eq. (24), we transform the latter equation into a rotating frame

$$\begin{aligned} W = & \exp \{ i[\omega_P A_{22} + (\omega_P + \omega_R) A_{33} \\ & + (\omega_P + \omega_R + \omega_M) A_{44} \\ & + (\omega_P + \omega_R + \omega_M - \omega_C) A_{55} \\ & + (\omega_P + \omega_R + \omega_M - \omega_C - \omega_A) A_{66}] t \} \\ & \exp \{ -i[\mathbf{k}_P \cdot \mathbf{r} A_{22} + (\mathbf{k}_P + \mathbf{k}_R) \cdot \mathbf{r} A_{33} \\ & + (\mathbf{k}_P + \mathbf{k}_R + \mathbf{k}_M) \cdot \mathbf{r} A_{44} \\ & + (\mathbf{k}_P + \mathbf{k}_R + \mathbf{k}_M - \mathbf{k}_C) \cdot \mathbf{r} A_{55} \\ & + (\mathbf{k}_P + \mathbf{k}_R + \mathbf{k}_M - \mathbf{k}_C - \mathbf{k}_A) \cdot \mathbf{r} A_{66}] \}. \end{aligned}$$

We assume that the central frequencies of all fields are resonant with the loop  $|1\rangle \leftrightarrow |2\rangle \leftrightarrow |3\rangle \leftrightarrow |4\rangle \leftrightarrow |5\rangle \leftrightarrow |6\rangle \leftrightarrow |1\rangle$ ,

$$\omega_P + \omega_R + \omega_M - \omega_C - \omega_A = \omega_L. \quad (25)$$



In addition, we impose the phase matching condition

$$\mathbf{k}_P + \mathbf{k}_R + \mathbf{k}_M - \mathbf{k}_C - \mathbf{k}_A = \mathbf{k}_L. \quad (26)$$

The transformed density operator  $\varrho = WRW^\dagger$  obeys the master equation

$$\partial_t \varrho = -\frac{i}{\hbar}[H, \varrho] + \mathcal{L}_\gamma \varrho, \quad (27)$$

and the transformed Hamiltonian  $H$  is

$$H = -\hbar \sum_{k=4}^6 \Delta_k A_{kk} - \hbar (\Omega_P A_{21} + \Omega_R A_{32} + \Omega_M A_{43} + \Omega_C A_{45} + \Omega_A A_{56} + \Omega_L A_{61} + \text{H.c.}). \quad (28)$$

In this equation,  $\Delta_k$   $k \in \{2, \dots, 6\}$  is a detuning defined as

$$\Delta_4 = \omega_P + \omega_R + \omega_M - \omega_4, \quad (29a)$$

$$\Delta_5 = \omega_P + \omega_R + \omega_M - \omega_C - \omega_5, \quad (29b)$$

$$\Delta_6 = \omega_L - \omega_6. \quad (29c)$$

The Rabi frequencies of the various fields are

$$\Omega_P = \frac{\mathbf{d}_{21} \cdot \mathbf{e}_P}{\hbar} \mathcal{E}_P, \quad (30a)$$

$$\Omega_R = \frac{\mathbf{d}_{32} \cdot \mathbf{e}_R}{\hbar} \mathcal{E}_R, \quad (30b)$$

$$\Omega_M = \frac{\mathbf{d}_{43} \cdot \mathbf{e}_M}{\hbar} \mathcal{E}_M, \quad (30c)$$

$$\Omega_C = \frac{\mathbf{d}_{45} \cdot \mathbf{e}_C}{\hbar} \mathcal{E}_C, \quad (30d)$$

$$\Omega_A = \frac{\mathbf{d}_{45} \cdot \mathbf{e}_A}{\hbar} \mathcal{E}_A, \quad (30e)$$

$$\Omega_L = \frac{\mathbf{d}_{51} \cdot \mathbf{e}_L}{\hbar} \mathcal{E}_L. \quad (30f)$$

Since  $\Omega_M$  and  $\Omega_L$  depend on position and time via the envelope functions  $\mathcal{E}_M$  and  $\mathcal{E}_L$ , the density operator  $\varrho$  in the rotating frame is a slowly varying function of  $\mathbf{r}$  and  $t$ . The propagation of the probe and control fields inside the medium is governed by Maxwell's equations. We only take into account  $\mathbf{E}_M$  and  $\mathbf{E}_L$  for the self-consistent Maxwell-Bloch equations. The P and R fields create coherent population trapping on the  $|1\rangle \leftrightarrow |2\rangle \leftrightarrow |3\rangle$  transition such that the atoms are in a dark state for these fields. After a transient time, the P and R fields will thus not experience absorption or dispersion. Furthermore, the auxiliary fields C and A are detuned from resonance and couple to states that are virtually empty (see Supplementary Section 'Analytical solution'). We can thus neglect their absorption and dispersion. The wave equation governing the propagation of the electric field  $\mathbf{E} = \mathbf{E}_M + \mathbf{E}_L$  is then given by

$$\left( \frac{1}{c^2} \partial_t^2 - \Delta \right) \mathbf{E} = -\frac{1}{c^2 \epsilon_0} \partial_t^2 \mathbf{P}. \quad (31)$$

The source term on the right hand side of Eq. (31) comprises the macroscopic polarisation  $\mathbf{P}$  induced by the external fields. We neglect atom-atom interactions such that  $\mathbf{P}$  can be expressed in terms of the single-atom polarisation,

$$\mathbf{P} = \mathcal{N}(\mathbf{d}_{34} R_{43} + \mathbf{d}_{16} R_{61} + \text{c.c.}). \quad (32)$$

In this equation,  $\mathcal{N}$  is the atomic density of the medium. Note that the coherences  $R_{43}$  and  $R_{61}$  in Eq. (32) are related to the coherences of the density operator  $\varrho$  in the rotating frame by

$$R_{43} = \varrho_{43} e^{i(\mathbf{k}_M \cdot \mathbf{r} - \omega_M t)}, \quad R_{61} = \varrho_{61} e^{i(\mathbf{k}_L \cdot \mathbf{r} - \omega_L t)}. \quad (33)$$

In the slowly varying envelope approximation [1] and with Eqs. (19) and (30), the wave equation (31) can be cast into the form

$$\left( \frac{1}{c} \partial_t + \hat{\mathbf{k}}_M \cdot \nabla \right) \Omega_M = i\eta_M \varrho_{43}, \quad (34a)$$

$$\left( \frac{1}{c} \partial_t + \hat{\mathbf{k}}_L \cdot \nabla \right) \Omega_L = i\eta_L \varrho_{61}, \quad (34b)$$

where  $\hat{\mathbf{k}}_X = \mathbf{k}_X/k_X$  denote unit vectors. The coupling constants  $\eta_M$  and  $\eta_L$  are given by

$$\eta_M = \frac{\mathcal{N} |\mathbf{d}_{43}|^2}{2\hbar \epsilon_0 c} \omega_M, \quad (35a)$$

$$\eta_L = \frac{\mathcal{N} |\mathbf{d}_{61}|^2}{2\hbar \epsilon_0 c} \omega_L, \quad (35b)$$

and  $c$  is the speed of light. In the case of  $\eta_L$  it is useful to replace the dipole moment through the radiative decay rate,

$$\eta_L = \frac{3\mathcal{N} \lambda_{61}^2}{8\pi} \gamma_{61}, \quad (36)$$

where  $\lambda_{61}$  is the wavelength of the atomic transition  $|6\rangle \leftrightarrow |1\rangle$ .

## VII. METHODS

Here we outline the analytical solution to the Maxwell-Bloch equations of our system. In a first step, we derive the adiabatic solutions for the atomic coherences  $\varrho_{43}$  and  $\varrho_{61}$ . To this end, we assume that the fields  $\Omega_M$  and  $\Omega_L$  are sufficiently weak and expand the atomic density operator as follows [2, 3],

$$\varrho = \sum_{k=0}^{\infty} \varrho^{(k)}, \quad (37)$$

where  $\varrho^{(k)}$  denotes the contribution to  $\varrho$  in  $k$ th order in the Hamiltonian

$$H_1 = -\hbar (\Omega_M A_{43} + \Omega_L A_{61}) + \text{H.c.} \quad (38)$$

The solutions  $\varrho^{(k)}$  can be obtained by re-writing the master equation (27) as

$$\mathcal{L}\varrho = \mathcal{L}_0\varrho - \frac{i}{\hbar}[H_1, \varrho], \quad (39)$$

where the linear super-operator  $\mathcal{L}_0$  is independent of  $\Omega_M$  and  $\Omega_L$ . Inserting the expansion (37) into Eq. (39) leads to the following set of coupled differential equations

$$\dot{\varrho}^{(0)} = \mathcal{L}_0\varrho^{(0)}, \quad (40)$$

$$\dot{\varrho}^{(k)} = \mathcal{L}_0\varrho^{(k)} - \frac{i}{\hbar}[H_1, \varrho^{(k-1)}]. \quad k > 0. \quad (41)$$

Equation (40) describes the interaction of the atom with the fields  $\Omega_P$ ,  $\Omega_R$ ,  $\Omega_C$  and  $\Omega_A$  to all orders and in the absence of  $H_1$ . Higher-order contributions to  $\varrho$  can be obtained if Eq. (41) is solved iteratively. Equations (40) and (41) must be solved under the constraints  $\text{Tr}(\varrho^{(0)}) = 1$  and  $\text{Tr}(\varrho^{(k)}) = 0$  ( $k > 0$ ).

We omit the small decay rate  $\Gamma$  of state  $|3\rangle$  and find that the zeroth order solution in steady state is given by the EIT dark state of the three-level ladder system  $|1\rangle$ ,  $|2\rangle$  and  $|3\rangle$ ,

$$\varrho_{11}^{(0)} = P_{11} = \frac{|\Omega_R|^2}{|\Omega_P|^2 + |\Omega_R|^2}, \quad (42a)$$

$$\varrho_{33}^{(0)} = P_{33} = \frac{|\Omega_P|^2}{|\Omega_P|^2 + |\Omega_R|^2}, \quad (42b)$$

$$\varrho_{13}^{(0)} = C_{13} = -\frac{\Omega_P^* \Omega_R^*}{|\Omega_P|^2 + |\Omega_R|^2}. \quad (42c)$$

For  $|\Omega_P| \ll |\Omega_R|$  the steady state is reached within several inverse decay times  $1/\gamma$ . Next we solve Eq. (41) for  $k = 1$  and obtain

$$\begin{aligned} \varrho^{(1)}(t) = & \frac{i}{\hbar} \mathcal{L}_0^{-1} [H_1(t), \varrho^{(0)}] \\ & - \frac{i}{\hbar} \mathcal{L}_0^{-1} \int_0^t dt' e^{\mathcal{L}_0(t-t')} \partial_{t'} \left( [H_1(t'), \varrho^{(0)}] \right), \end{aligned} \quad (43)$$

where we assumed  $H_1(0) = 0$ . If  $H_1(t)$  varies sufficiently slowly with time, the second term on the right-hand side in Eq. (43) involving the time derivative of  $H_1$  can be neglected. More precisely, this approximation is justified if the bandwidth  $\delta_\nu$  of the pulses  $\Omega_M$  and  $\Omega_L$  is small as compared to the relevant differences between eigenfrequencies of  $H_0$ . Through a numerical study we find that this condition is satisfied if all detunings  $\Delta_k$  ( $k \in \{4, 5, 6\}$ ) and the Rabi frequencies  $\Omega_R$ ,  $\Omega_C$  and  $\Omega_A$  are large as compared to the bandwidth  $\delta_\nu$ . The analytical expression for the first-order density operator  $\varrho$  is too bulky to display here.

For stationary fields the spatial distribution of  $\Omega_M$  and  $\Omega_L$  is determined by the matrix exponential in Eq. (13)

of the main text. We find [4]

$$\begin{aligned} \exp(i\mathcal{M}z) = & \exp(ia_0z) \\ & \left[ \cos\left(\sqrt{\mathbf{a}^2}z\right) \mathbf{1} + i \frac{\mathbf{a} \cdot \boldsymbol{\sigma}}{\sqrt{\mathbf{a}^2}} \sin\left(\sqrt{\mathbf{a}^2}z\right) \right], \end{aligned} \quad (44)$$

where  $\mathbf{1}$  is the  $2 \times 2$  identity matrix,  $\sigma_k$  are the Pauli matrices and

$$a_0 = \frac{1}{2} \text{Tr}(\mathcal{M}), \quad \mathbf{a} = \frac{1}{2} \text{Tr}(\mathcal{M}\boldsymbol{\sigma}). \quad (45)$$

Complete conversion of  $\Omega_M$  into  $\Omega_L$  or vice versa occurs if  $\exp(i\mathcal{M}z)$  has only off-diagonal elements at some position  $z_0$ ,

$$\exp(i\mathcal{M}z_0) = \begin{pmatrix} 0 & c_1 \\ c_2 & 0 \end{pmatrix}, \quad (46)$$

with some constants  $c_1$  and  $c_2$ . A necessary condition for this to occur is that the term proportional to  $a_z \sigma_z$  in Eq. (44) vanishes. Since  $a_z \propto \mathcal{M}_{11} - \mathcal{M}_{22}$ , we thus conclude that the diagonal elements of  $\mathcal{M}$  must be equal for complete conversion. Furthermore, if the diagonal elements of  $\mathcal{M}$  are non-zero, the pre-factor  $\exp(ia_0z)$  in Eq. (44) with  $a_0 \propto \mathcal{M}_{11} + \mathcal{M}_{22}$  will in general result in an exponential damping of the fields. Efficient and coherent conversion can thus be achieved if the matrix elements of  $\mathcal{M}$  vanish, i.e., if  $\chi_{43}^{(M)} = \chi_{61}^{(L)} = 0$ . By analysing the full expressions of the first-order results for the coherences  $\varrho_{43}$  and  $\varrho_{61}$ , we find that  $\chi_{43}^{(M)} \approx \chi_{61}^{(L)} \approx 0$  can be achieved for

$$\Delta_5 = \frac{|\Omega_C|^2}{\Delta_4}, \quad (47a)$$

$$\Delta_6 = \frac{|\Omega_A|^2}{\Delta_5} = \Delta_4 \frac{|\Omega_A|^2}{|\Omega_C|^2}. \quad (47b)$$

With these conditions, the first-order susceptibilities in Eq. (44) of the main text are given by

$$\chi_{43}^{(M)} \approx i\beta, \quad \chi_{43}^{(L)} \approx \alpha, \quad (48a)$$

$$\chi_{61}^{(M)} \approx \alpha^*, \quad \chi_{61}^{(L)} \approx ig, \quad (48b)$$

where

$$\alpha = \frac{\Omega_C}{\Delta_4 \Omega_A^*} C_{13}, \quad (49a)$$

$$\beta = \frac{\gamma}{2} \frac{|\Omega_C|^2}{\Delta_4^2 |\Omega_A|^2} P_{33}, \quad (49b)$$

$$g = \frac{\Gamma}{2|\Omega_A|^2} \left( 1 + 2 \frac{|\Omega_C|^2}{\Delta_M^2} \right) P_{11}. \quad (49c)$$

In the following we assume  $|\Omega_R| \gg |\Omega_P|$  such that  $P_{11} \approx 1$ ,  $|C_{13}| \approx |\Omega_P/\Omega_R|$  and  $P_{33} \approx |C_{13}|^2$ . The matrix exponential  $\exp(i\mathcal{M}z)$  with  $\mathcal{M}$  determined by Eqs. (48) and (49) can be calculated via Eqs. (44) and (45). The solution for  $\boldsymbol{\Omega}(z)$  in Eq. (15) of the main text is then obtained by assuming  $\alpha > 0$ ,  $\varepsilon \ll 1$  and  $\varepsilon_\Gamma/\varepsilon \ll 1$ , where  $\varepsilon$  and  $\varepsilon_\Gamma$  are defined in Eq. (16) of the main text.

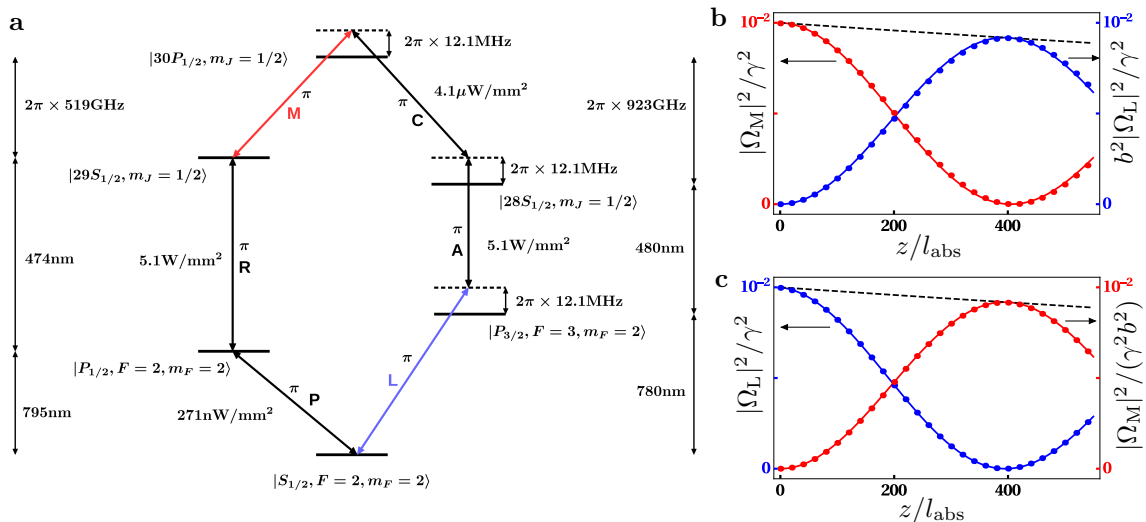


FIG. 5. Implementation of the scheme in Rb. **a** Realisation of the level scheme in Fig. 1 of the main text based on transitions in  $^{87}\text{Rb}$ . All quantum numbers of the employed states as well as intensities, polarisations and detunings are indicated. Note that energy spacings are not to scale. **b** and **c** show the intensities of the fields  $\Omega_M$  (red) and  $\Omega_L$  (blue) inside the medium for the parameters in **a**. Dots indicate the results from a numerical integration of Maxwell-Bloch equations. **b** A CW millimeter wave enters the medium at  $z = 0$ . The intensity of the microwave field at  $z = 0$  is  $1.4\text{nW}/\text{mm}^2$ . The intensity of the optical output field at  $z = 400l_{\text{abs}}$  is  $897.5\text{nW}/\text{mm}^2$ . **c** A CW optical field enters the medium at  $z = 0$ . The intensity of the optical input field at  $z = 0$  is  $994.2\text{nW}/\text{mm}^2$ . The intensity of the microwave field at  $z \approx 10l_{\text{abs}}$  is  $1.1\text{nW}/\text{mm}^2$ . The decay rate  $\gamma = 2\pi \times 6.1\text{MHz}$  corresponds to the D<sub>2</sub> line. We set the decay rate  $\Gamma$  of all Rydberg states equal to the decay rate of the  $|28S_{1/2}\rangle$  state at  $T = 300\text{K}$ , which is faster than the decay rate of the  $|30P_{1/2}\rangle$  state. We find [5]  $\Gamma/\gamma = 1/508$  and the ratio of the single-photon Rabi frequencies is  $b = \sqrt{0.97}$ .

### VIII. LEVEL SHIFTS

Here we provide a quantitative estimate for the level shifts  $\Delta_{\text{vdW}}$  and  $\Delta_{\text{DD}}$  that are induced by the van der Waals and dipole-dipole interactions, respectively. The magnitude of these shifts strongly depends on the distance between atom pairs. The probability density function  $w$  for the distance  $r$  between nearest neighbours in a random distribution of particles is given by [6],

$$w(r) = \frac{3}{a} \left(\frac{r}{a}\right)^2 \exp\left[-\left(\frac{r}{a}\right)^2\right], \quad (50)$$

where

$$a = \left[\frac{3}{4\pi\mathcal{N}}\right]^{1/3} \quad (51)$$

is the Wigner-Seitz radius and  $\mathcal{N}$  is the density of particles. We consider an atomic density of  $\mathcal{N} = 3 \times 10^{17}\text{m}^{-3}$  which can be routinely achieved in cold atom experiments. For the considered parameters in Sec. II of the main text, the population of all Rydberg states is of the order of  $10^{-3}$ . It follows that the density of Rydberg excitations is  $\mathcal{N}_{\text{R}} = 3 \times 10^{14}\text{m}^{-3}$ . In order to estimate the impact of the frequency shifts at this density of Rydberg excitations, we evaluate  $\Delta_{\text{vdW}}$  and  $\Delta_{\text{DD}}$  at the distance  $R_{90}$  where 90% of all Rydberg atom pairs will have a

larger separation than  $R_{90}$ ,

$$0.9 = \int_{R_{90}}^{\infty} w(r) dr. \quad (52)$$

For  $\mathcal{N}_{\text{R}} = 3 \times 10^{14}\text{m}^{-3}$  we find  $R_{90} \approx 3.44\mu\text{m}$ . We begin with a discussion of the van der Waals shifts  $\Delta_{\text{vdW}}$  for  $ns - ns$  Rydberg atom pairs. We evaluate  $\Delta_{\text{vdW}}$  based on the results in [7] and for different principal quantum numbers  $n$ . The results are shown in Tab. I and illustrate that these shifts are of the order of 10kHz for  $n \lesssim 35$ . Next we consider the shifts induced by the resonant dipole-dipole interaction. The magnitude of  $\Delta_{\text{DD}}$  depends crucially on the quantum numbers of the involved states. In order to illustrate this, we first assume that the transition  $|3\rangle \leftrightarrow |4\rangle$  involves the states  $|3\rangle = |30S_{1/2}, m_J = 1/2\rangle$  and  $|4\rangle = |30P_{1/2}, m_J = 1/2\rangle$ . At  $R_{90}$ , we find [8]

$$\Delta_{\text{DD}} \propto \frac{1}{4\pi\epsilon_0\hbar} \frac{|\langle 3|\hat{\mathbf{d}}|4\rangle|^2}{R_{90}^3} \approx 2\pi \times 0.92\text{MHz}, \quad (53)$$

$n$	20	30	35	40
$\Delta_{\text{vdW}}/(2\pi)$ [kHz]	0.065	3.84	27.23	104.96

TABLE I. Van der Waals shifts  $\Delta_{\text{vdW}}$  for  $ns - ns$  atom pairs separated by  $R_{90}$ .

where  $\hat{\mathbf{d}}$  is the electric dipole operator. On the other hand, the value of  $\Delta_{\text{DD}}$  reduces dramatically by choosing a transition  $(n-1)s \leftrightarrow np$  between Rydberg states with different principal quantum numbers. For example, by choosing  $|\tilde{3}\rangle = |29S_{1/2}, m_J = 1/2\rangle$  instead of  $|3\rangle = |30S_{1/2}, m_J = 1/2\rangle$ , we get

$$\Delta_{\text{DD}} \propto \frac{1}{4\pi\epsilon_0\hbar} \frac{|\langle\tilde{3}|\hat{\mathbf{d}}|4\rangle|^2}{R_{90}^3} \approx 2\pi \times 12.0\text{kHz}, \quad (54)$$

which is two orders of magnitude smaller as compared to the  $ns \leftrightarrow np$  transition in Eq. (53). More values for  $\Delta_{\text{DD}}$  are summarised in Tab. II.

$n$	20	30	35	40
$\Delta_{\text{DD}}/(2\pi)[\text{MHz}]$ $ns \leftrightarrow np$	0.15	0.92	1.81	3.21
$\Delta_{\text{DD}}/(2\pi)[\text{kHz}]$ $(n-1)s \leftrightarrow np$	1.77	12.0	24.1	43.4

TABLE II. Resonant dipole-dipole shifts  $\Delta_{\text{DD}}$  for atom pairs separated by  $R_{90}$ .

## IX. EXAMPLE SYSTEM

Here we present a worked example based on an atomic ensemble of  $^{87}\text{Rb}$  atoms. The atomic level scheme is

shown in the Supplementary Fig. 5a. The optical field L couples to the  $D_2$  line, and the auxiliary P field couples to the  $D_1$  line. The intensities and detunings are chosen such that they match the parameters in Sec. II of the main text. The transition dipole matrix elements for the optical transitions can be found in [9], and for transitions between Rydberg states we employ the method outlined in [8].

The intensities inside the medium for conversion of stationary fields is shown in the Supplementary Figs. 5b and c. The conversion efficiency at  $l = 400l_{\text{abs}}$  is 91.75%. In contrast to Sec. II of the main text, we set the decay rate  $\Gamma$  equal to the decay rate of the  $|28S_{1/2}\rangle$  state at  $T = 300\text{K}$ . This results in a slightly larger ratio  $\Gamma/\gamma$  compared with Sec. II of the main text, and hence the conversion efficiency is slightly smaller.

For an atomic density of  $\rho = 3 \times 10^{17}\text{m}^{-3}$ , the absorption length is  $l_{\text{abs}} = 3.43 \times 10^{-2}\text{mm}$ , and hence full conversion occurs for a medium length of  $l \approx 13.7\text{mm}$ . The length needed for full conversion can be reduced by increasing the density of atoms or by using a different atomic transition  $|1\rangle \leftrightarrow |6\rangle$  with an enhanced dipole matrix element. For example, the experiment in [10] reports an optical depth of 1000 for cold Rb atoms in a cylindrical trap geometry of length  $l = 4.6\text{mm}$ . From Sec. VIII we find that  $\Delta_{\text{vdW}}$  and  $\Delta_{\text{DD}}$  at  $R_{90}$  are significantly smaller than the bandwidth  $\Delta\nu$  of the conversion scheme, and hence the reduction of the conversion efficiency due to Rydberg-Rydberg interactions will be small.

- 
- [1] M. O. Scully and M. S. Zubairy, *Quantum Optics* (Cambridge University Press, Cambridge, 1997)
- [2] M. Kiffner and K.-P. Marzlin, Phys. Rev. A **71**, 033811 (2005)
- [3] M. Kiffner, U. Dorner, and D. Jaksch, Phys. Rev. A **85**, 023812 (2012)
- [4] C. Cohen-Tannoudji, B. Diu, and F. Laloë, *Quantum Mechanics (Volume I)* (J. Wiley & Sons, London, 1977)
- [5] I. I. Beterov, I. I. Ryabtsev, D. B. Tretyakov, and V. M. Entin, Phys. Rev. A **79**, 052504 (2009)
- [6] S. Chandrasekhar, Rev. Mod. Phys. **15**, 1 (1943)
- [7] K. Singer, J. Stanojevic, M. Weidemüller, and R. Cote, Journal of Physics B: Atomic, Molecular and Optical Physics **38**, S295 (Jan. 2005), ISSN 0953-4075, <http://iopscience.iop.org/0953-4075/38/2/021>
- [8] T. G. Walker and M. Saffman, Phys. Rev. A **77**, 032723 (2008)
- [9] Daniel A. Steck, “Rubidium 87 D Line Data,” available online at <http://steck.us/alkalidata> (revision 2.1.4, 23 December 2010).
- [10] B. Sparkes, J. Bernu, M. Hosseini, J. Geng, Q. Glorieux, P. Altin, P. Lam, N. Robins, and B. Buchler, in *Journal of Physics: Conference Series*, Vol. 467 (IOP Publishing, 2013) p. 012009